Various Crack Concepts for Curved Fracture in Concrete

J. G. ROTS

TNO Institute for Building Materials and Structures, Computational Mechanics Dept., P.O. Box 49, NL-2600 AA Delft, The Netherlands

ABSTRACT

The performance of smeared crack concepts and discrete crack concepts for simulating curved fracture in concrete is investigated. The differences between fixed, multi-directional and rotating crack approaches are discussed. It is furthermore shown that smeared analyses lead to stress-locking.

KEYWORDS

fracture, cracking, concrete, softening, mixed-mode, stress-locking, smeared, discrete

INTRODUCTION

Tensile failure in matrix-aggregate composites like concrete involves progressive micro-cracking, tortuous debonding and other processes of internal damage. These processes eventually coalesce into a geometrical discontinuity that separates the material. Such a discontinuity is called a crack. Undoubtedly, the discrete crack concept is the approach that reflects this phenomenon most closely. It directly models the crack via a displacement-discontinuity in an interface element that separates two solid elements. Unfortunately, the approach does not fit the nature of the finite element displacement method and it is computationally more convenient to employ a smeared crack concept. A smeared approach imagines the cracked solid to be a continuum and permits a description in terms of stress-strain relations. However, here the converse drawback occurs, since the underlying assumption of displacement continuity conflicts with the realism of a *dis*continuity.

To date, there is no consensus on the question which type of approach should be preferred. The confusion is even worse since the class of smeared crack concepts itself already offers a variety of possibilities, ranging from fixed single to fixed multi-directional and rotating smeared crack approaches. Here, the distinction lies in the orientation of the crack, which is either kept constant, updated in a stepwise manner or updated continuously.

It is the purpose of this paper to investigate the merits and demerits of the various approaches. On purpose we utilize the term 'curved fracture' instead of 'mixed-mode fracture', since there is no consensus on the question whether mixed-mode fracture exists for heterogeneous materials like concrete. Aside from cases of extremely high mode II or mode III intensity - which are beyond the scope of the paper - the relevant experiments reveal that curved fractures are predominantly of the mode I type (Arrea & Ingraffea, 1982, Jenq & Shah, 1988, Kobayashi *et al.*, 1985).

DISCRETE CRACK CONCEPT

The discrete crack concept models a crack by means of a separation between element edges (Ngo & Scordelis, 1967). The approach implies a continuous change in nodal connectivity and constrains the crack to follow a path along the element edges. For general purposes this is not exactly attractive, but a number of special purposes exist for which the drawbacks can be circumvented. This is particularly the case if we employ smeared approaches as a *predictor* of the crack path, whereafter a *corrector* analysis is made on a mesh in which a potential discrete crack is predefined according to the smeared prediction. For such problems one may predefine interface elements in the original mesh, keeping the topology preserved. The initial stiffness of the elements is assigned a large dummy value in order to simulate the uncracked state with rigid connection between overlapping nodes. Upon violating a condition of crack initiation, the element stiffness is changed and a constitutive model for discrete cracks is mobilized. Such a model links the tractions $\mathbf{t}^{cr}$ to the relative displacements $\mathbf{u}^{cr}$ via C^{cr} which represents phenomena like softening:

$$\Delta \mathbf{t} = C^{cr} \Delta \mathbf{u}^{cr} \tag{1}$$

FIXED SINGLE SMEARED CRACK CONCEPT

A consistent way to set-up a fixed smeared crack concept is to decompose the global strain increment $\Delta\boldsymbol{\varepsilon}$ into a part $\Delta\boldsymbol{\varepsilon}^{cr}$ of the crack and a part $\Delta\boldsymbol{\varepsilon}^{co}$ of the solid material between the cracks (de Borst & Nauta, 1985, Rots *et al.*, 1985):

$$\Delta\boldsymbol{\varepsilon} = \Delta\boldsymbol{\varepsilon}^{cr} + \Delta\boldsymbol{\varepsilon}^{co} \tag{2}$$

This opens up the possibility to treat the constitutive behavior of the crack separately from the constitutive behavior of the concrete. For the concrete we can for instance insert the elasticity matrix, while for the crack the smeared analogy of (1) can be defined in the local crack coordinate system:

$$\Delta \mathbf{t}^{cr} = \mathbf{D}^{cr} \Delta \mathbf{e}^{cr} \tag{3}$$

in which $\Delta\mathbf{t}^{cr}$ contains the mode I normal traction t_n and the mode II shear traction t_t, and $\Delta\mathbf{e}^{cr}$ contains the mode I crack normal strain ε_{nn}^{cr} and the mode II crack shear strain γ_{nt}^{cr}. The local crack strain increment $\Delta\mathbf{e}^{cr}$ is related to the global crack strain vector $\Delta\boldsymbol{\varepsilon}^{cr}$ via a transformation matrix that reflects the orientation of the *fixed* crack.

FIXED MULTI-DIRECTIONAL SMEARED CRACK CONCEPT

The strategy of strain-decomposition allows for a sub-decomposition of the crack strain into the separate contributions of a number of multi-directional cracks that simultaneously occur at a sampling point, i.e.

$$\Delta\boldsymbol{\varepsilon}^{cr} = \Delta\boldsymbol{\varepsilon}_1^{cr} + \Delta\boldsymbol{\varepsilon}_2^{cr} + \dots\dots\dots \tag{4}$$

where $\Delta\boldsymbol{\varepsilon}_1^{cr}$ is the global crack strain increment owing to a primary crack, $\Delta\boldsymbol{\varepsilon}_2^{cr}$ is the global crack strain increment owing to a secondary crack and so on. Each of these (fixed) cracks is assigned its own local crack strain vector $\mathbf{e}_i^{cr}$, its own traction vector $\mathbf{t}_i^{cr}$, its own transformation matrix and its own traction-strain matrix $\mathbf{D}_i^{cr}$. By assembling these individual vectors and matrices, the overall stress-

strain relation for the multiply cracked solid can be set up analogously to the relation for a singly cracked solid (de Borst & Nauta, 1985). The multi-directional crack concept is applicable to conditions where the fracture starts in tension and subsequently proceeds in tension-shear. This behavior generally implies that the axes of principal stress rotate after crack formation. For such cases, the use of fixed single cracks leads to an increasing discrepancy between the axes of principal stress and the fixed crack axes. The fixed multi-directional crack concept provides an alternative. Whenever the angle of inclination between the existing crack(s) and the current direction of principal stress exceeds the value of a certain *threshold angle* α, a new crack may be initiated. In this way, we end up with a system of *non-orthogonal* cracks, as pioneered by de Borst & Nauta (1985).

ROTATING SMEARED CRACK CONCEPT

A prominent feature of the fixed single and fixed multi-directional crack concepts is the inclusion of an *explicit* shear term for the fixed plane(s). Unfortunately, the identity "shear" does not provide much insight in the behavior of structures. Designers as well as researchers prefer to think in terms of "principal stress", the axes of which continuously rotate after cracking. This poses a need to monitor stress-strain relations in the rotating principal coordinate system, instead of in the fixed crack system. Consistent use of such rotating principal stress-strain relations requires principal stress and strain to be coaxial. This coaxiality can be achieved only via an *implicit* shear term in the rotating principal 1,2 reference frame (Bazant, 1983, Willam *et al.*, 1987):

$$G_{12} = \frac{(\sigma_{11} - \sigma_{22})}{2(\varepsilon_{11} - \varepsilon_{22})} \tag{5}$$

It is intriguing to make contact between this so-called rotating crack concept and the fixed multi-directional crack concept. Assuming the threshold angle for multi-directional cracks to vanish, we observe that a new fixed crack arises at each stage of the incremental process. Hence, the continuously-rotating crack concept can be interpreted as the limiting case of the fixed multi-directional crack concept for a zero threshold angle, which has certain advantages (Rots, 1988a).

ELASTIC-SOFTENING CONSTITUTIVE MODEL

For tension and tension-shear dominated separation an adequate model is constructed by assuming elasticity for the concrete and softening for the crack. Specifically, C^{cr} of (1) for discrete cracks and $\mathbf{D}^{cr}$ of (3) for smeared cracks can be assumed to be of the form:

$$C^{cr} = \begin{bmatrix} C^I & 0 \\ 0 & C^{II} \end{bmatrix} \tag{6}$$

$$D^{cr} = \begin{bmatrix} D^I & 0 \\ 0 & D^{II} \end{bmatrix} \tag{7}$$

The assumption of zero off-diagonal terms implies that *direct* shear-normal coupling across a fixed plane has been ignored. It will be demonstrated that this is justified since a similar phenomenon can be obtained *indirectly*, by allowing for crack rotation. The mode I stiffness moduli C^I and D^I are defined by three tensile softening parameters: the tensile strength f_{ct}, the fracture energy G_f and the shape of the softening diagram. For a discrete crack, this relation can be worked out exactly (Hillerborg *et al.*, 1976), whereas for a smeared crack a fourth factor enters the scene, viz. the crack band width h (Bazant & Oh, 1983), which is related to the particular finite element configuration (Rots *et al.*, 1985, Rots, 1988a). As mentioned before, the mode II stiffness moduli C^{II} and D^{II} will *not* be set-up in the spirit of mode II or mixed-mode fracture. Rather, these will be defined with a view to capturing stress rotations. For the discrete crack concept, stress rotation occurs in the elastic elements at either side of the discontinuity. Hence, any mode II phenomena can be constrained from the analysis, so that C^{II} has been set equal to zero after cracking. For smeared cracks D^{II} is highly essential as it controls the stress rotation in cracked elements. It is illustrative to relate this modulus to the classical shear retention factor β (Suidan & Schnobrich, 1973) via

$$\frac{1}{\beta G}=\frac{1}{G}+\frac{1}{D^{II}} \quad \rightarrow \quad D^{II}=\frac{\beta}{1-\beta}G \tag{8}$$

in which G is the elastic shear modulus. In this paper, numerical experiments will be undertaken on three formulations:

— β=0, i.e. D^{II}=0. This implies zero shear transfer and no stress rotation.

— β=0.05, i.e. $D^{II}\approx 0.053G$. This is the traditional method of some constant shear retention factor.

—

$$\beta=\left[1-\frac{\varepsilon_{nn}^{cr}}{\varepsilon_{u}^{cr}}\right]^{p} \tag{9}$$

with p some constant and ε_u^{cr} being the ultimate strain of the softening diagram. This degradation of β from 1 (full retainment of elastic shear) to zero, corresponds to a degradation of D^{II} from infinite (full interlock) to zero. This somewhat reflects that aggregate interlock diminishes with increasing crack opening.

For the extension towards multi-directional cracks, the reader is referred to Rots (1988a). Essentials in this respect are that the energy consumed in previous defects is subtracted from the energy available for the current defect, and that the variable shear retention factor is made a function of the principal crack strain ε_{11}^{cr}, representing the damage in all cracks, instead of ε_{nn}^{cr} for a single crack. The further extension towards rotating cracks lies in a zero threshold angle α and in the coaxiality-enforcing shear term of (5). βG along the "currently-active crack' must be taken in accordance with this shear term.

TENSION-SHEAR MODEL PROBLEM

To illustrate the gradual transition from fixed single, fixed multi-directional to rotating cracks, we consider a tension-shear model problem. It concerns an elastic-softening continuum of unit dimensions with E=10000 N/mm^2, ν=0.2, f_{ct}=1.0 N/mm^2 and a linear strain-softening diagram with an ultimate strain ε_u^{cr} that equals three times the elastic strain at peak-strength, i.e. ε_u^{cr}=0.0003, corresponding to G_f=0.15 J/m^2 over unit crack band width h=1.0 mm. Initially, the continuum is subjected to tensile straining in the x-direction accompanied by lateral Poisson contraction in the y-direction, i.e. $\Delta\varepsilon_{xx} : \Delta\varepsilon_{yy} : \Delta\gamma_{xy} = 1 : -\nu : 0$. Immediately after cracking, a switch is made to combined biaxial tension and shear according to $\Delta\varepsilon_{xx} : \Delta\varepsilon_{yy} : \Delta\gamma_{xy} = 0.5 : 0.75 : 1$, involving the axes of principal strain to continuously rotate after crack formation. This scheme is shown in Fig. 1 and was inspired by Willam *et al.* (1987). The focus is placed on a variation of the threshold angle α, while the mode II relation across the currently-active crack is kept fixed in the form of a quadratic degradation of β according to (9) with p=2 (different crack shear relations do not affect the basic conclusions). The adopted values of α range from 0, 7.5, 15, 30, 45 up to 90 degrees. The extreme of α=0^o corresponds to a continuously rotating crack (not maintaining coaxiality, however) and the other extreme of α=90^o corresponds to a fixed single-crack. In addition, the problem was analyzed using the coaxial rotating crack model, i.e. for threshold angle α=0^o and βG enforcing coaxiality according to (5).

The nominal τ_{xy}–γ_{xy} shear response predicted is shown in Fig. 2. The two computations for a zero threshold angle provide the most flexible response. In addition, these two computations show curves that are nicely smooth as a result of the continuously changing orientation of the crack. Upon increasing the threshold angle the response becomes less flexible and we observe increasing discontinuity as a result of the interval adaptation of the currently-active crack orientation to the continuous rotation of principal stress. For threshold angles beyond 45^o the initiation of inclined cracks is postponed even

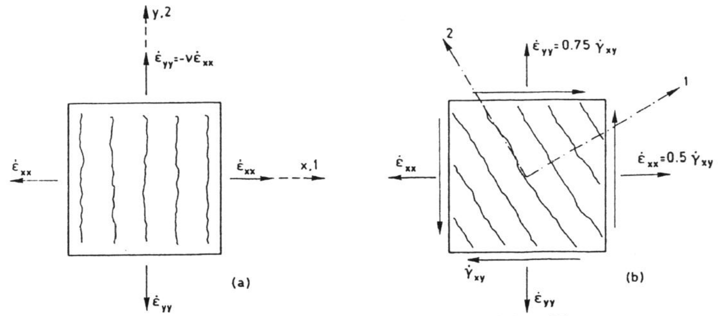

Fig. 1. Lay-out of tension-shear model problem.
(a) tension up to cracking; (b) biaxial tension with shear beyond cracking

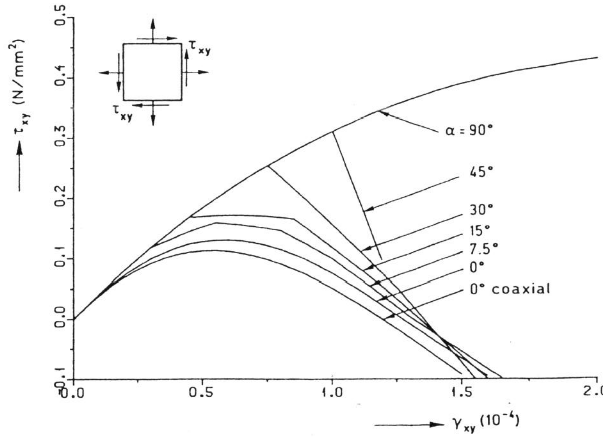

Fig. 2. Shear stress-strain response of model problem in x,y direction, for different threshold angles α between multi-directional cracks.

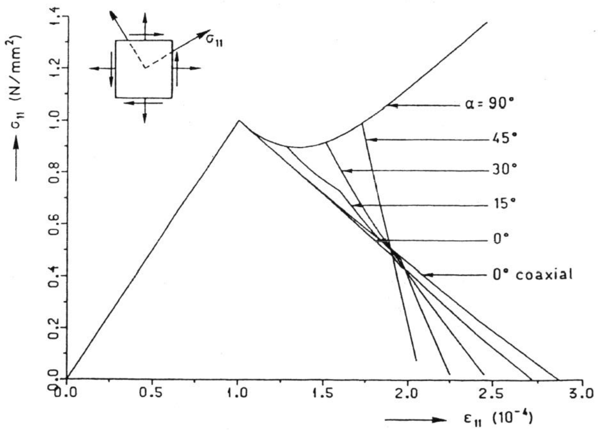

Fig. 3. Principal tensile stress-strain response of model problem in 1,2 direction, for different threshold angles α between multi-directional cracks.

further and the solution approaches the fixed single-crack solution for α=90°, which is extremely stiff. This observation of stiff behavior for fixed-single cracks corresponds to previous findings (Balakrishnan & Murray, 1987, Crisfield & Wills, 1987, Willam *et al.*, 1987). The present results indicate that a crack-strain decreasing shear retention function does not provide a remedy. However, it is intriguing that the results in Fig. 2 for threshold angles less than 90° invariably do display shear softening along the x,y-plane of initial cracking. *This shear softening occurs implicitly, as a consequence of the crack rotation.* In a similar way, it can be shown that implicit shear-normal coupling occurs as a consequence of crack rotation (Rots, 1988a).

Fig. 3 shows the principal tensile stress σ_{11} versus principal tensile strain ε_{11}. The fixed-single crack curve (α=90°) is very illustrative as it shows σ_{11} to decrease only slightly beyond crack initiation, whereafter it re-starts to increase and amply exceeds the tensile strength. On decreasing the threshold angle, inclined cracks arise and the tensile strength is correctly kept under control, which is reflected by the truncation of the fixed single crack curve. It is concluded that crack rotation is an effective strategy for achieving a flexible response that correctly keeps the principal tensile stress under control.

SINGLE-NOTCHED SHEAR BEAM

To investigate whether the above conclusions also hold for structural fracture in element assemblies, we consider a single-notched shear beam which fails in curved mode I fracture (Arrea & Ingraffea, 1982). For details of the idealization and loading procedure, the reader is referred to Rots (1988a). We will confine attention here to the extreme cases of fixed single and/or orthogonal cracks (i.e. a high threshold angle) and coaxial rotating cracks. Five computations will be compared:

- fixed cracks, α=60°, $\beta\approx0$ (in fact 0.001 to avoid numerical problems)
- fixed cracks, α=60°, β=0.05
- fixed cracks, α=60°, variable β according to (9) with p=2
- coaxial rotating cracks, i.e. α=0, β enforcing coaxiality according to (5)
- predefined discrete crack, zero shear stiffness and zero shear tractions.
  Its location was adapted to the average of the smeared crack prediction.

A curve-fitting of the experimental result has not been undertaken. Rather, we will concentrate on an objective match between the smeared crack results and the discrete crack result. The elastic-softening parameters were taken as: E=24800 N/mm^2, ν=0.18, f_{ct}=2.8 N/mm^2, G_f=100 J/m^2, h=12mm and concave softening (Reinhardt *et al.*, 1986). Fig. 4 gives the load F versus the CMSD. Figs. 5 and 6 show the deformed meshes and principal stress plots for a typical smeared crack result and the discrete crack result.

All smeared crack results are too stiff in the post-peak regime. Only fixed cracks with $\beta\approx0$ and coaxial rotating cracks appear capable of producing a distinct softening response. Fixed cracks with significant shear retention fail in this respect. The latter statement already holds for a β value of 0.05, which is low compared to what is commonly used in engineering practice. The result for β=0.05 shows far too less structural softening. For the variable shear retention factor that decreases with increasing crack strain, or any other high shear retention factor, the response becomes even worse as no softening is predicted at all.

The fact that fixed smeared cracks perform adequately only in conjunction with a zero or almost zero shear retention factor is surprising, yet explainable. Such a model in which crack shear tractions remain zero or almost-zero, implies the axes of principal stress to be fixed or practically fixed after crack formation. Stress rotation is then caused by the surrounding elastic elements, while any rebuild of principal tensile stress in the cracked elements is constrained to occur parallel to the first crack. Non-zero shear retention factors provide an additional possibility of rebuilding principal tensile stress, via rotation in an inclined direction. *Whenever such an additional opportunity of stress rebuild is given, it is eagerly utilized.* This provides a straightforward extension of the conclusion from the above model problem. A further parallel with the model problem is that crack rotation remedies the overstiff

behavior, because the maximum principal tensile stress is correctly kept under control.

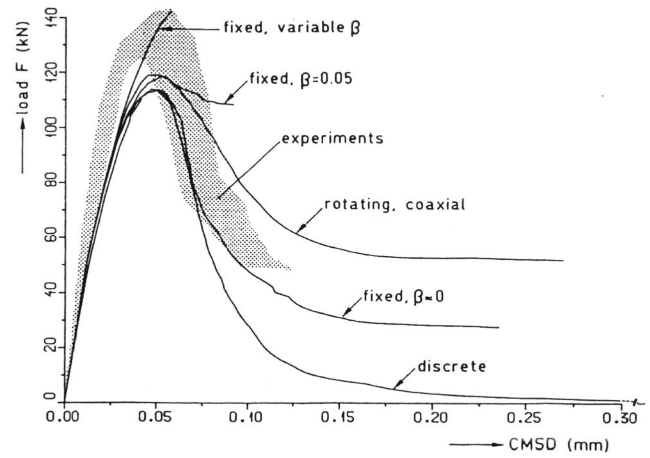

Fig. 4. Load F versus CMSD of single-notched shear beam.

It is striking that even the two best possible smeared crack results (fixed cracks with $\beta\approx0$ and coaxial rotating cracks) do not produce softening down to zero. Instead, they produce an incorrect residual load plateau. Softening down to zero could only be achieved via the computation on the discrete crack. To trace the causes, Fig. 6 gives an impression of the principal tensile stresses and their rotation, both for the smeared cracks (coaxial rotating; the plots for fixed cracks were even worse) and for the discrete crack. For the discrete crack we observe that the stress-plot is undisturbed and that the stresses at either side of the separation correctly come down to zero, which is in agreement with the physical process. With the smeared crack results, however, we observe significant tensile stresses at either side of the separation. This is incorrect. This phenomenon cannot be removed by further refinements in the smeared crack concept or the constitutive models. Instead, this *stress-locking is a fundamental consequence of the finite element displacement compatibility in the smeared softening approach.* Because of compatibility, a smeared cracked element will cause the adjacent uncracked elements to be strained as well. This strain in the adjacent elements causes the locked-in stresses, which explains the too stiff response. The discrete crack concept starts from displacement *in*compatibility and does not suffer from the phenomena (Figs. 5b, 6b). Full details about the generality and the seriousness of these issues have been given in recent publications (Rots, 1988a, Rots, 1988b).

CONCLUSIONS

- When smeared approaches are used, the coaxial rotating crack concept and the fixed crack concept with negligible shear retention (i.e. zero mode II stiffness) provide the best possible results. Fixed cracks with significant shear retention lead to very severe stress rebuild and uncontrollable stress rotations.
- The need for crack rotation and simple, implicit mode II terms contrasts with the aims of experimental researchers who generally pursue sophisticated, explicit mode II and mixed-mode crack laws for a fixed plane.
- When geometrical *discontinuities* are modeled using the assumption of displacement *continuity*, the finite element results will suffer from stress-locking. This is a serious phenomenon which calls for a revaluation of the discrete crack concept.

ACKNOWLEDGEMENTS

The discussions with Prof. J. Blaauwendraad and Prof. R. de Borst of Delft University of Technology are gratefully acknowledged. Examples were prepared using the DIANA finite element system of the TNO Institute for Building Materials and Structures.

REFERENCES

Arrea M. and A.R. Ingraffea (1982). Mixed-mode crack propagation in mortar and concrete. Report 81-13, Dept. Struct. Engng., Cornell Univ., Ithaca, NY.

Balakrishnan S. and D.W. Murray (1987). Prediction of response of concrete beams and panels by nonlinear finite element analysis. *IABSE Reports* 54, Coll. Comp. Mech. of Reinforced Concrete, Delft Univ. Press, 393-404.

Bazant Z.P. and B.H. Oh (1983). Crack band theory for fracture of concrete. *Mat. and Struct.*, RILEM, 16(93), 155-177.

Bazant Z.P. (1983). Comment on orthotropic models for concrete and geomaterials. *J. Engng. Mech.*, ASCE, 109(3), 849-865.

de Borst R. and P. Nauta (1985). Non-orthogonal cracks in a smeared finite element model. *Engng. Computations* 2, 35-46.

Crisfield M.A. and J. Wills (1987). Numerical comparisons involving different 'concrete-models'. *IABSE Reports* 54, Coll. Comp. Mech. of Reinforced Concrete, Delft Univ. Press, 177-187.

Hillerborg A., Modeer M. and P.E. Petersson (1976). Analysis of crack formation and crack growth in concrete by fracture mechanics and finite elements. *Cem. and Concr. Res.* 6(6), 773-782.

Jenq Y.S. and S.P. Shah (1988). Mixed-mode fracture of concrete. *Int. J. of Fracture.*

Kobayashi A.S., Hawkins M.N., Barker D.B. and B.M. Liaw (1985). Fracture process zone of concrete. Application of Fracture Mechanics to Cementitious Composites, Shah S.P. (Ed.), Martinus Nijhoff Publ., Dordrecht, 25-50.

Ngo D. and A.C. Scordelis (1967). Finite element analysis of reinforced concrete beams. *J. Am. Concrete Inst.* 64(14), 152-163.

Reinhardt H.W., Cornelissen H.A.W. and D.A. Hordijk (1986). Tensile tests and failure analysis of concrete. *J. Struct. Engng.*, ASCE, 112(11), 2462-2477.

Rots J.G., Nauta P., Kusters G.M.A. and J. Blaauwendraad (1985). Smeared crack approach and fracture localization in concrete. *HERON* 30(1), 1-48.

Rots J.G. (1988a). Computational modeling of concrete fracture. *Dissertation,* Delft Univ. of Techn., Dept. of Civil Engineering.

Rots J.G. (1988b). Stress rotation and stress locking in smeared analysis of separation. Proc. Int. Workshop on Fracture toughness and fracture energy - Test methods for concrete and rock, H. Mihashi (ed.), Tohoku University, Sendai, Japan.

Suidan M. and W.C. Schnobrich (1973). Finite element analysis of reinforced concrete. *J. Struct. Div.*, ASCE, 99(10), 2109-2122.

Willam K., Pramono E. and S. Sture (1987). Fundamental issues of smeared crack models. Proc. SEM-RILEM Int. Conf. on Fracture of Concrete and Rock, S.P. Shah and S.E. Swartz (Eds.), SEM, Bethel, 192-207.

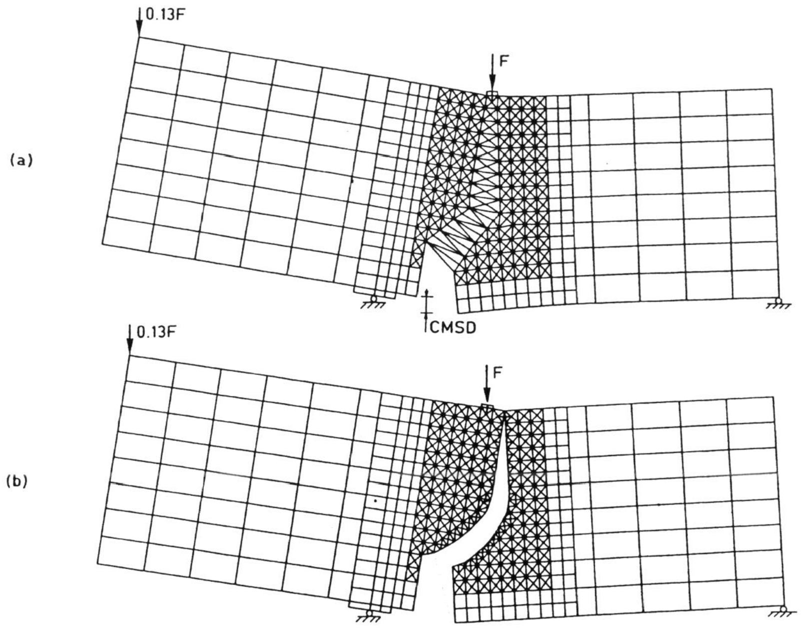

Fig. 5. Deformed meshes for single-notched shear beam at final stage.
(a) Localization for smeared cracks (coaxial, rotating).
(b) Genuine separation for predefined discrete crack.

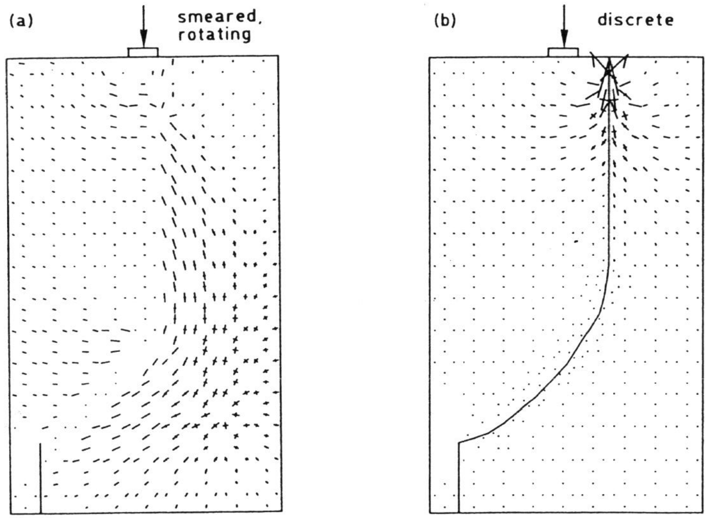

Fig. 6. Principal tensile stresses for single-notched shear beam at final stage.
(a) Stress-locking for smeared cracks (coaxial, rotating).
(b) Correct stress relief at either side of predefined discrete crack.